

Figure 3.18 Results of oedometer tests.

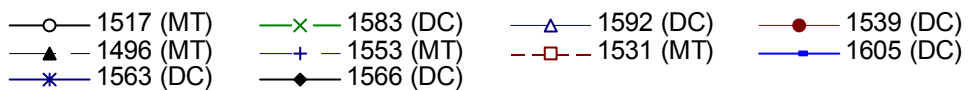
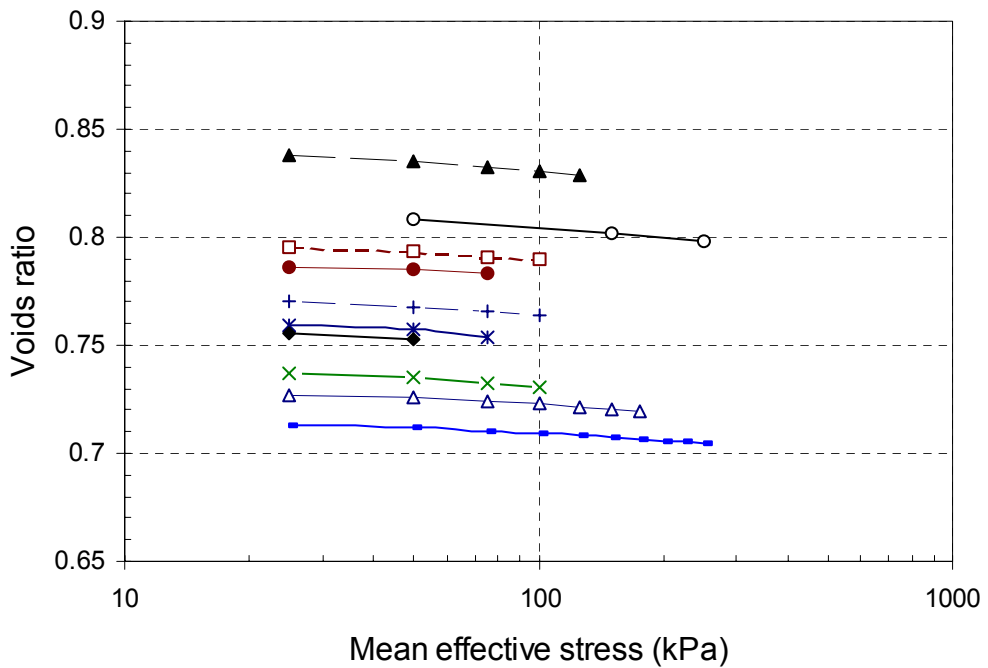
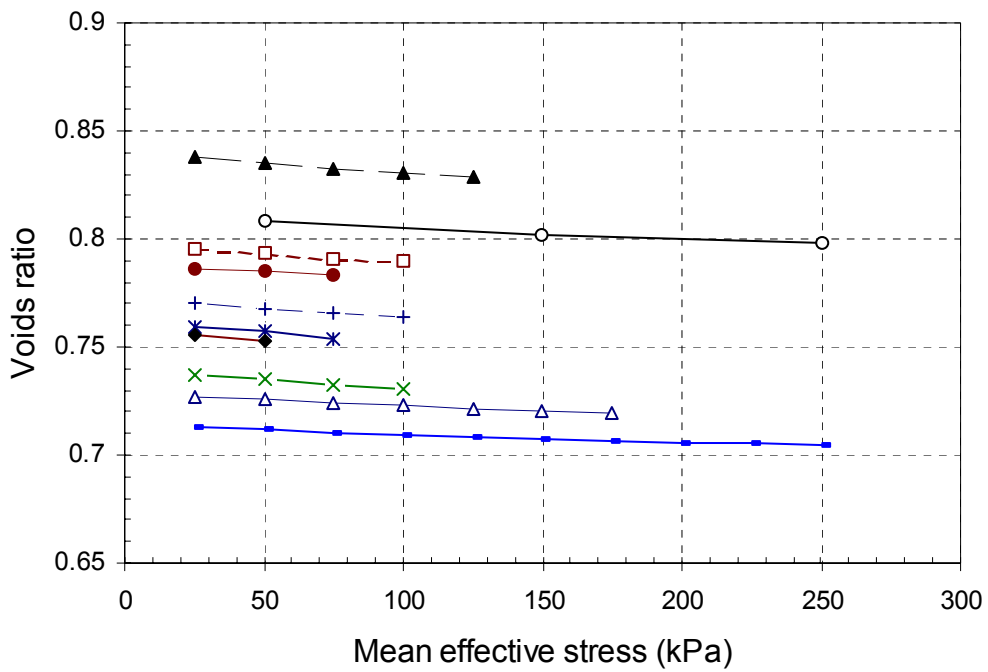
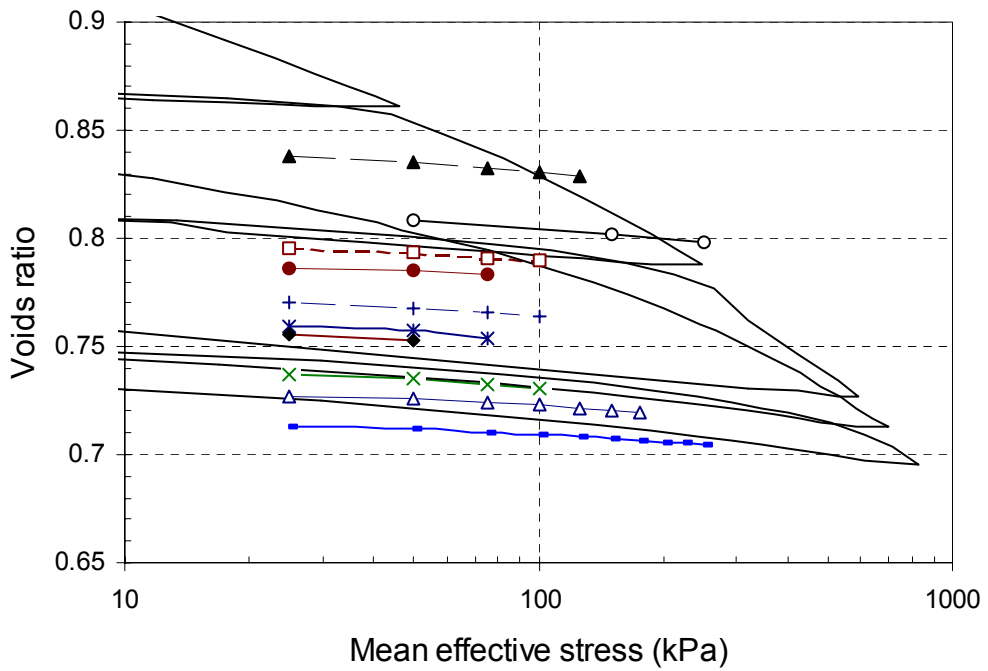
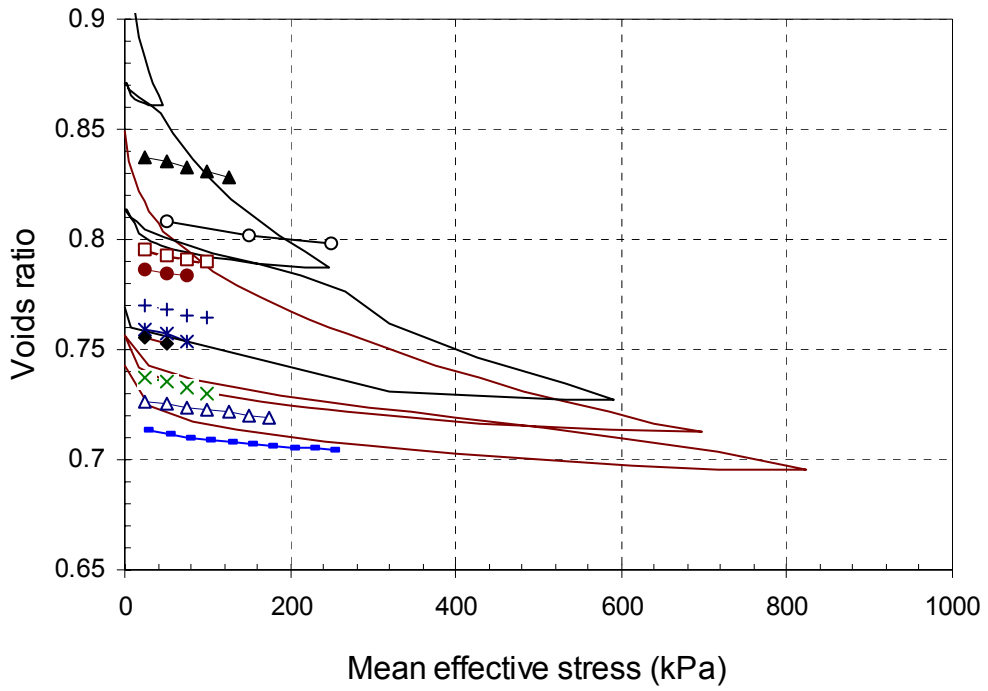


Figure 3.19 Results of the isotropic compression tests.



- | | | |
|-----------------|-----------------------|-----------------|
| ○ — 1517 (MT) | — x — 1583 (DC) | — △ — 1592 (DC) |
| ● — 1539 (DC) | — ▲ — 1496 (MT) | — + — 1553 (MT) |
| — □ — 1531 (MT) | — ● — 1605 (DC) | — * — 1563 (DC) |
| — ◆ — 1566 (DC) | — — — Oedometer tests | |

Figure 3.20 Results of the isotropic compression and oedometer tests.

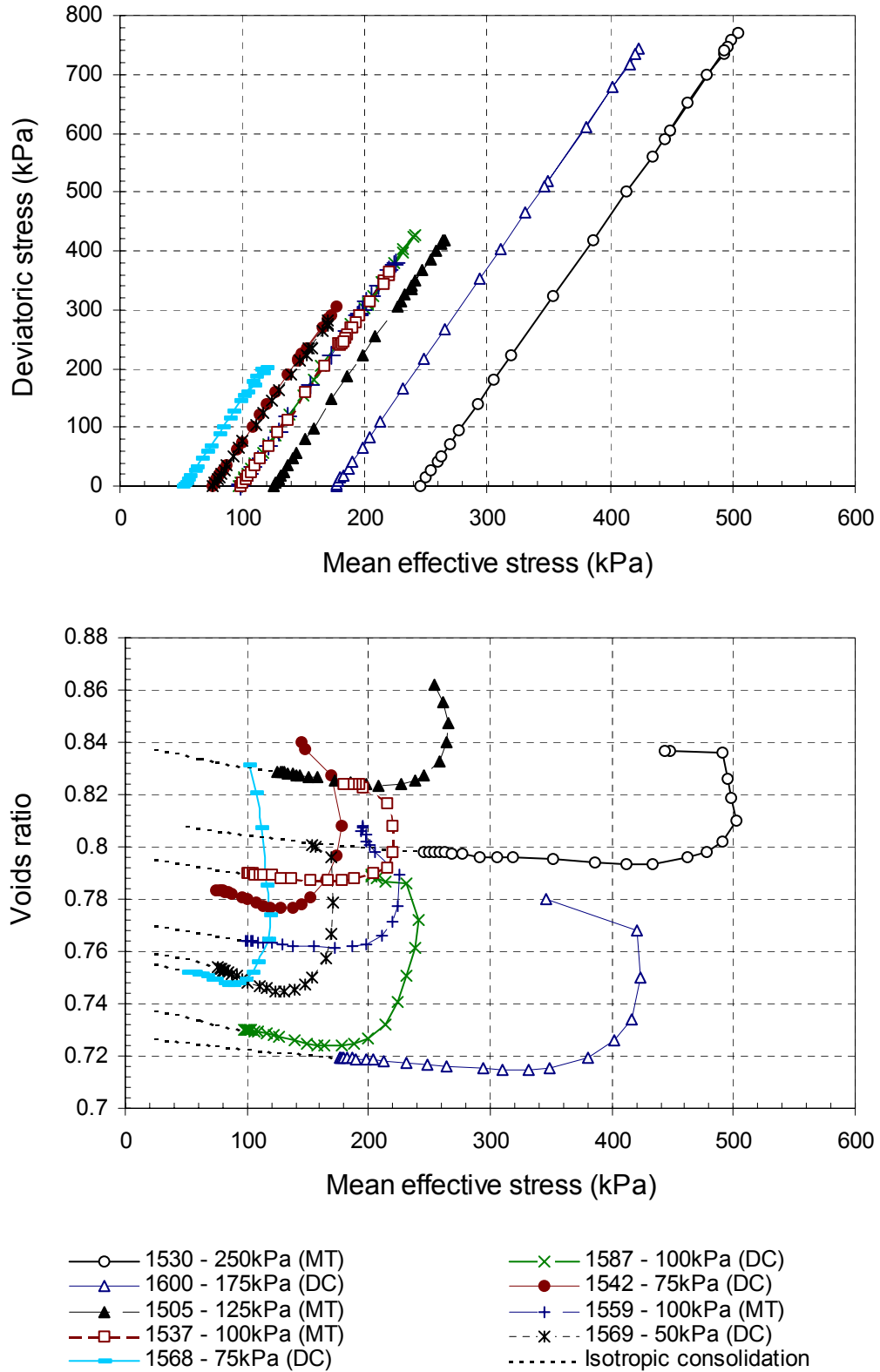


Figure 3.22 Results of the drained triaxial tests – q' and e vs. p' .

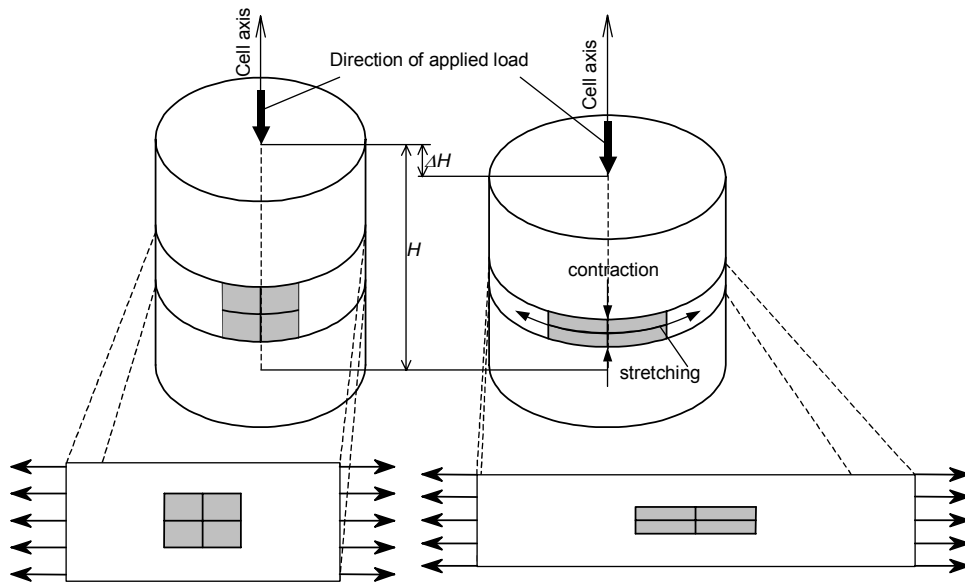


Figure 3.23 Illustration of uniaxial stress condition imposed on membranes in geocells.

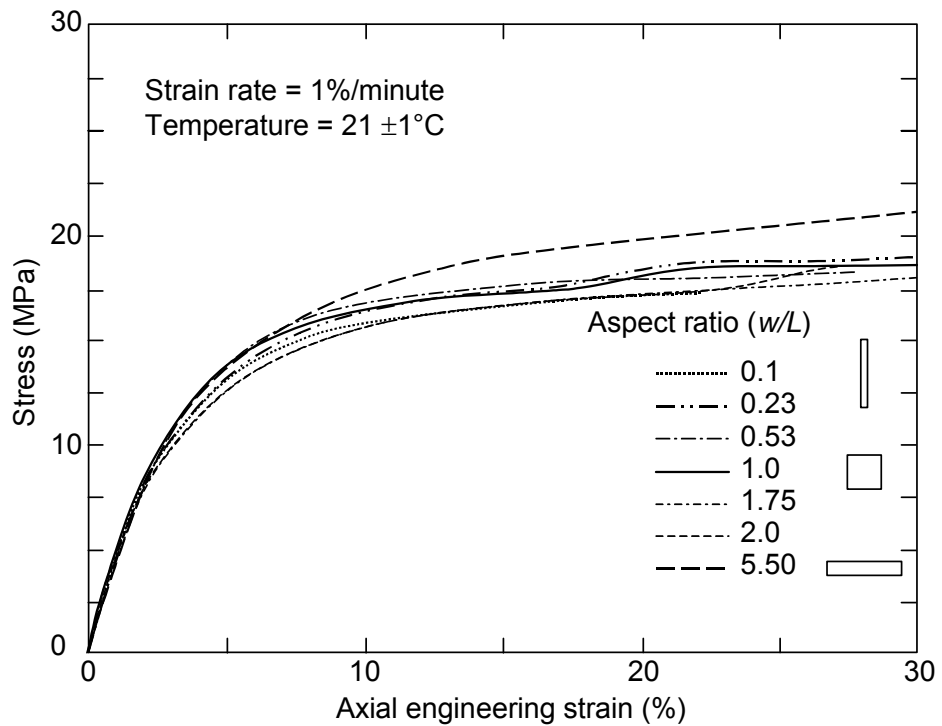


Figure 3.24 Comparison of uniaxial tension test results with different aspect ratios for HDPE geomembrane specimens (Merry and Bray 1996).

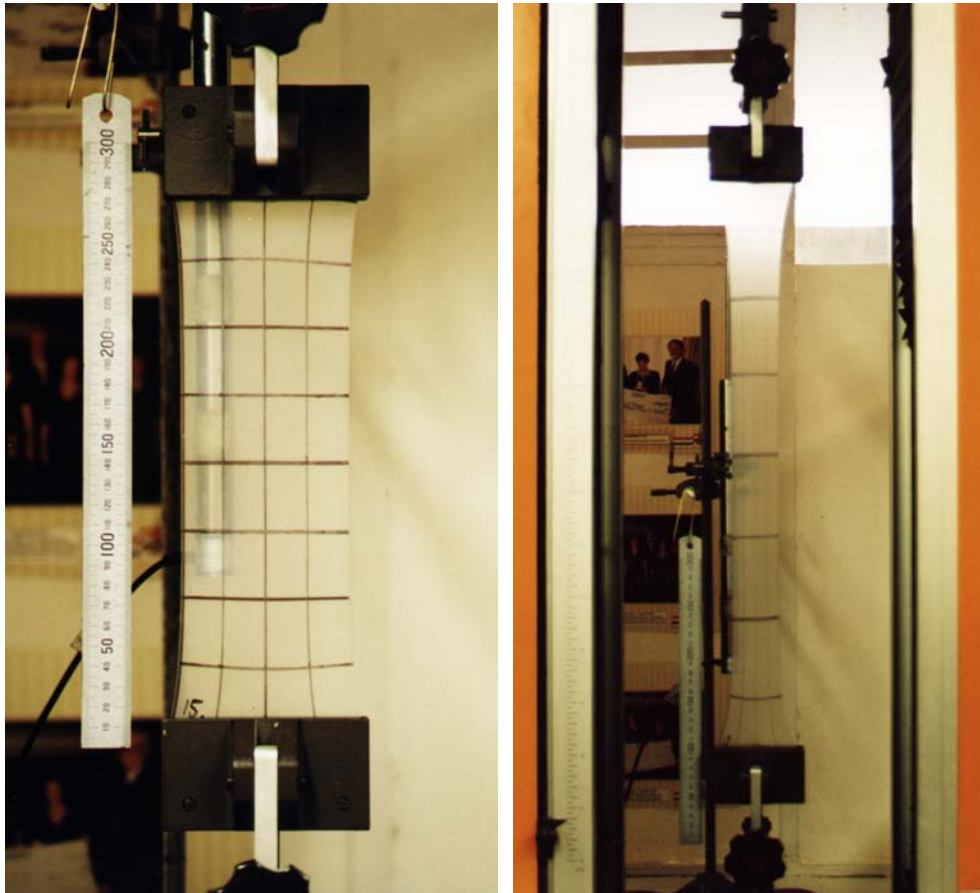


Figure 3.25 Photographs of membrane specimens in the test machine.

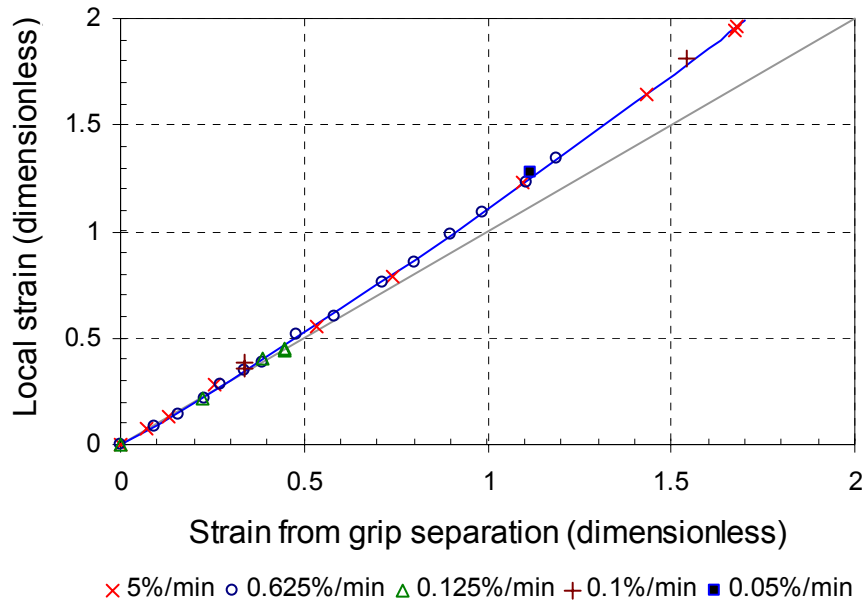


Figure 3.26 Local strain compared to strain calculated from grip separation.

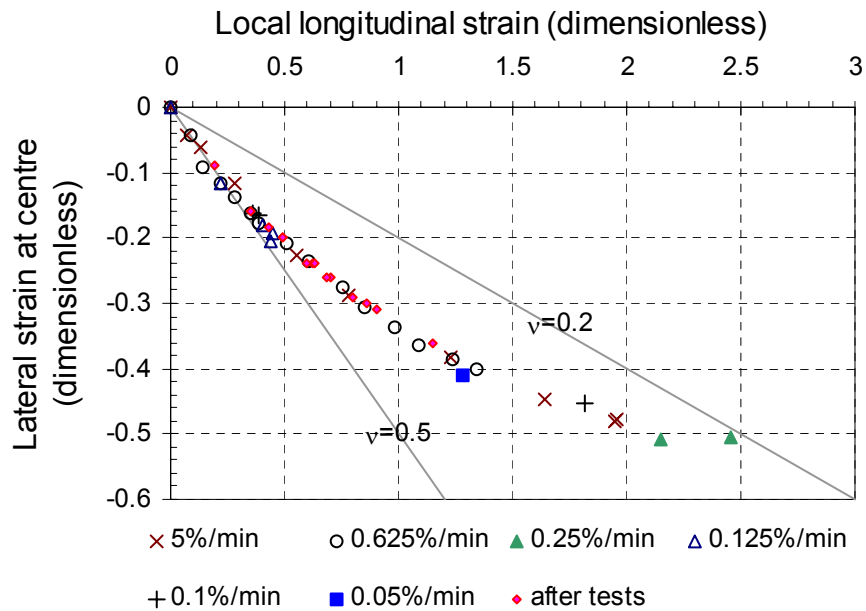


Figure 3.27 Local lateral strain compared to local longitudinal strain.

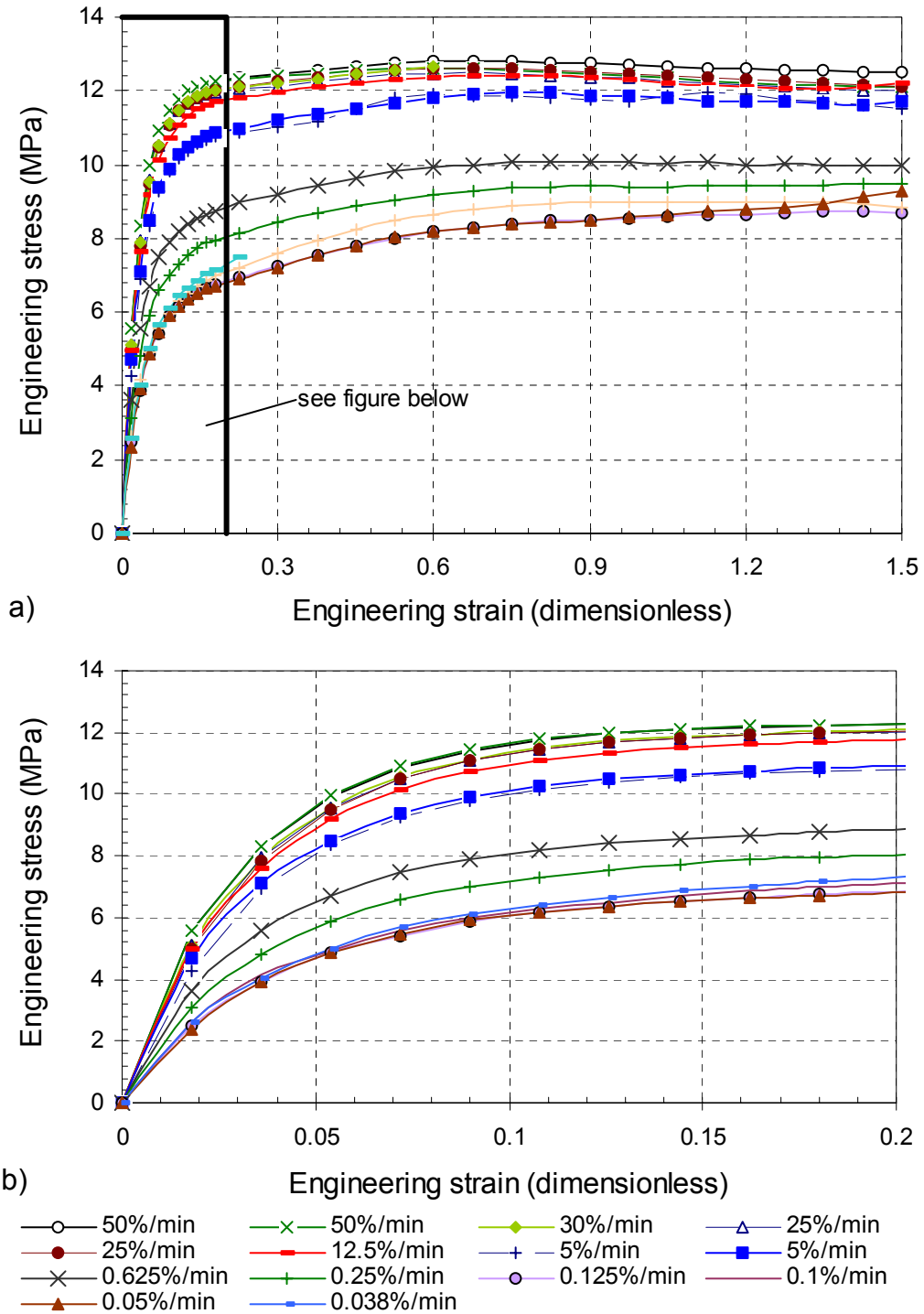


Figure 3.28 Results of uniaxial tensile tests on HDPE membrane assuming a constant cross-sectional area.



Figure 3.29 Instrumentation for measuring the circumferential strain of the specimens.

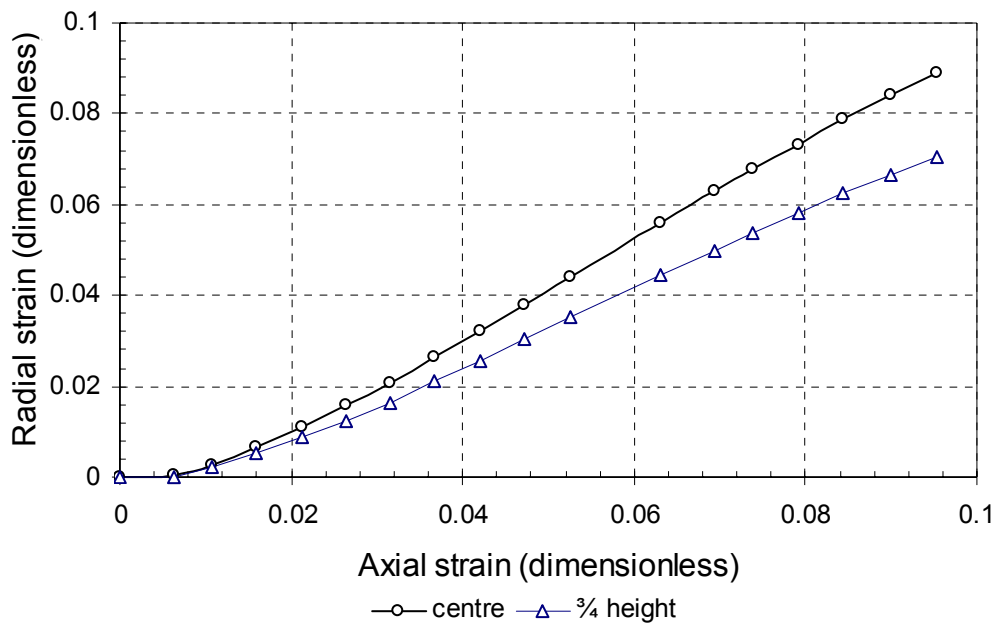


Figure 3.30 Radial strain measurements for first single cell compression test (Test 0).



Figure 3.31 Single cell specimen in test machine.

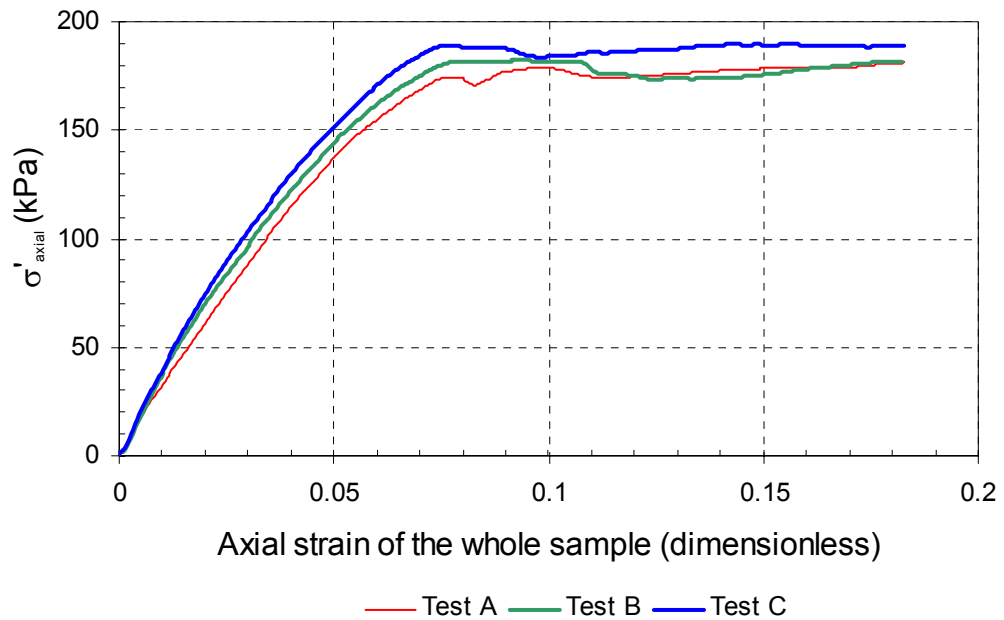


Figure 3.32 The stress-strain response of the single geocell compression tests.

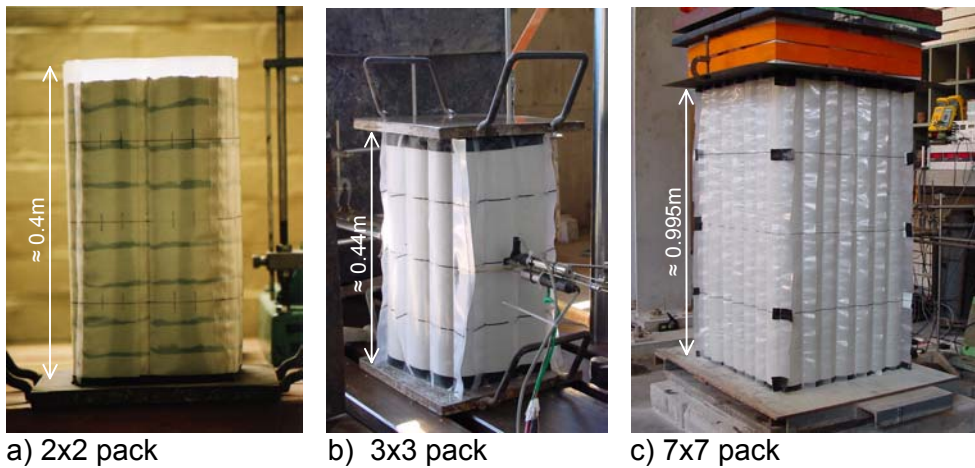
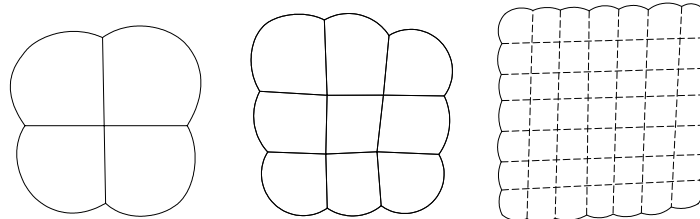


Figure 3.33 The tested multi-cell packs.

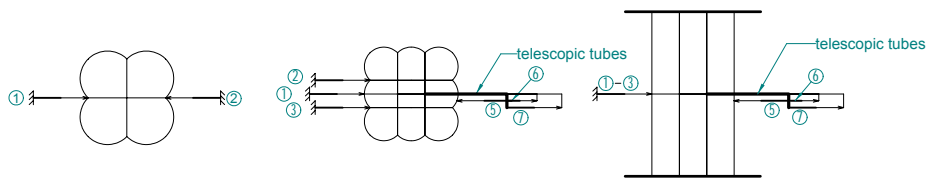


a) Top surface of 2x2 cell pack

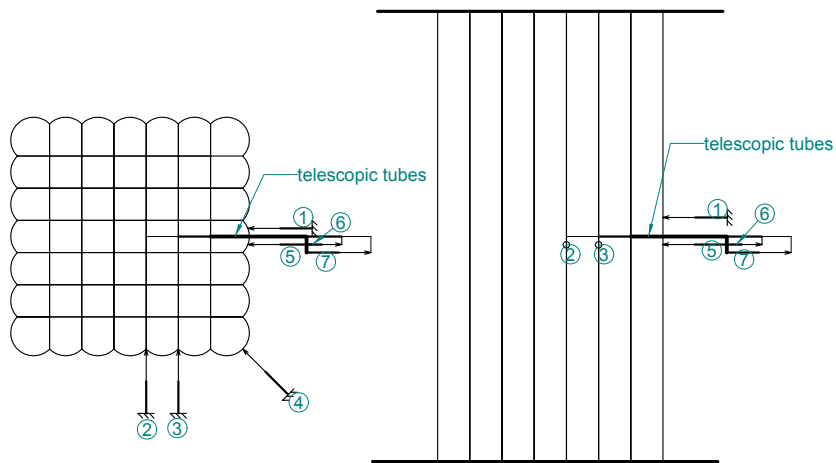


b) Cross sectional geometries reconstructed from measurements

Figure 3.34 Pack geometries showing straight inner membranes and bubble shaped outer membranes.



a) 2x2 and 3x3 cell packs



b) 7x7 cell pack



c) 7x7 cell pack

Figure 3.35 Arrangement of instrumentation on the tested 2x2, 3x3 and 7x7 cell packs.

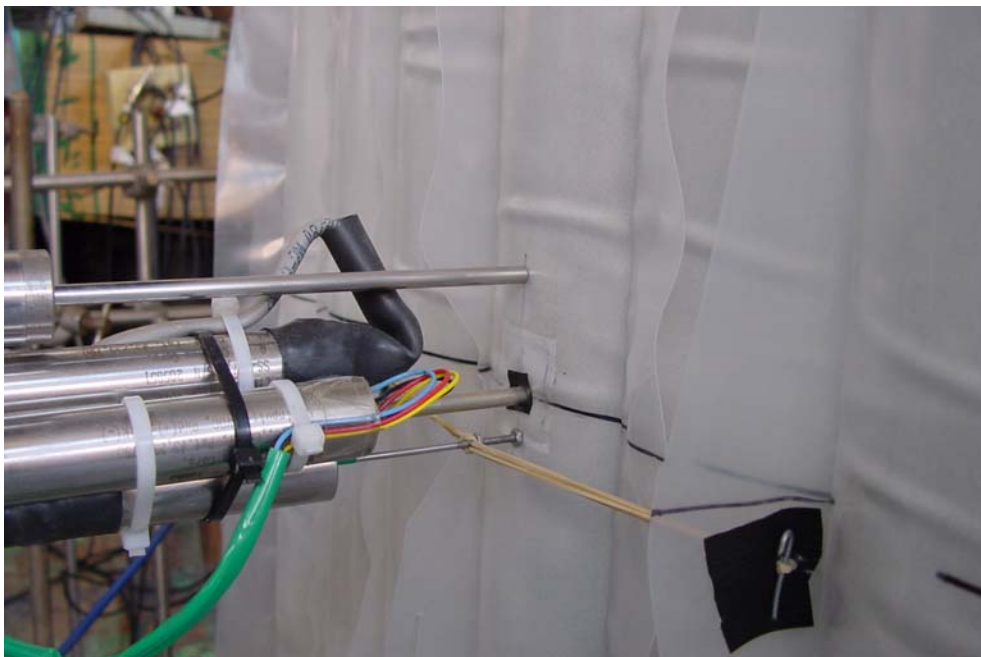
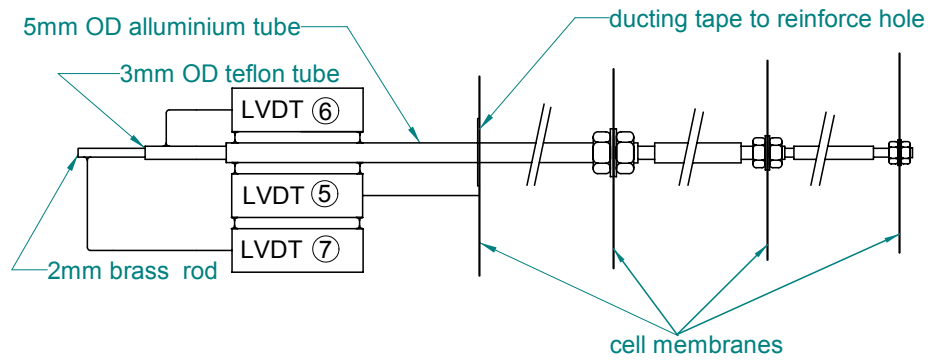


Figure 3.36 The "internal" LVDT system.

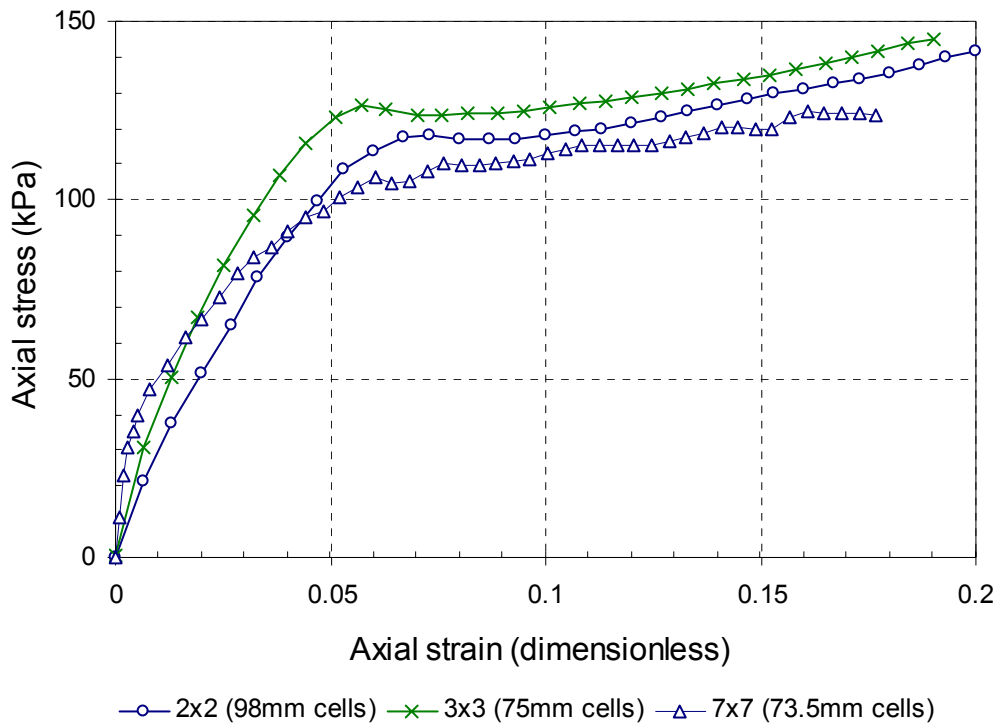


Figure 3.37 Stress-strain results of multi-cell tests (results in terms of engineering stress and strain).

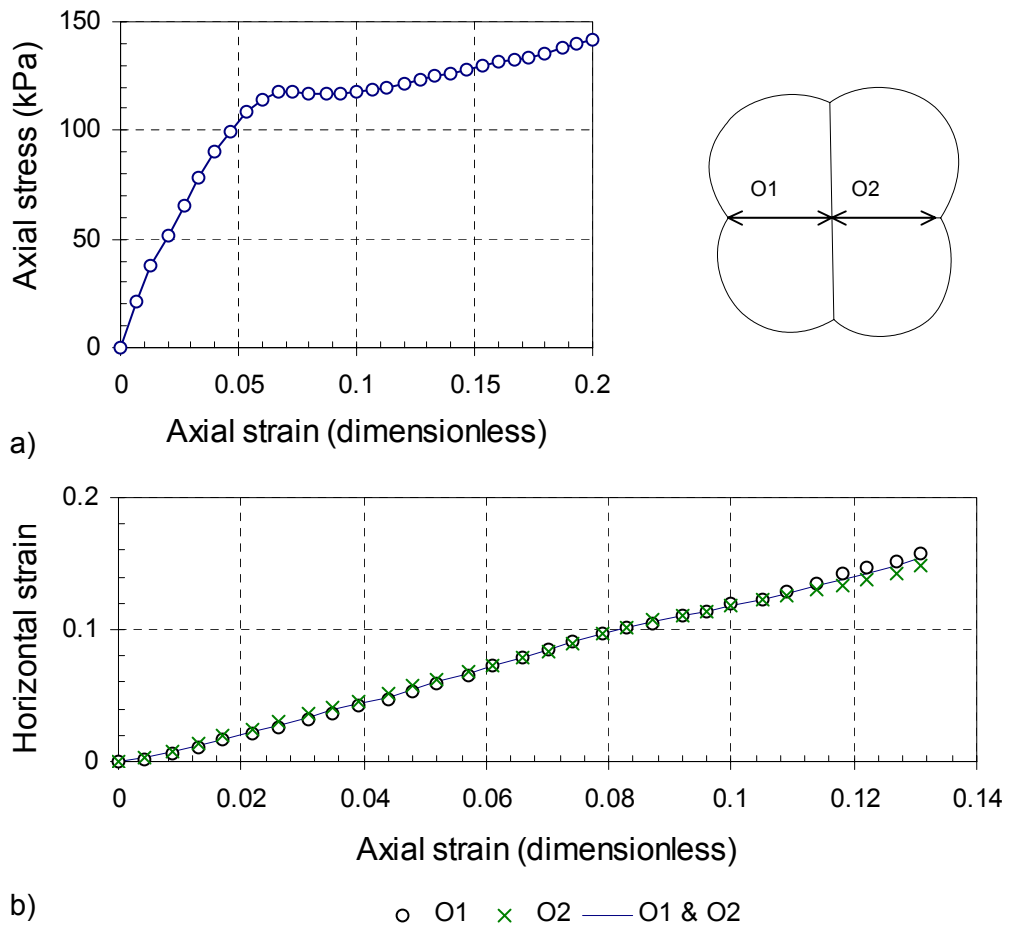


Figure 3.38 Results of the compression test on the 2x2 cell pack.

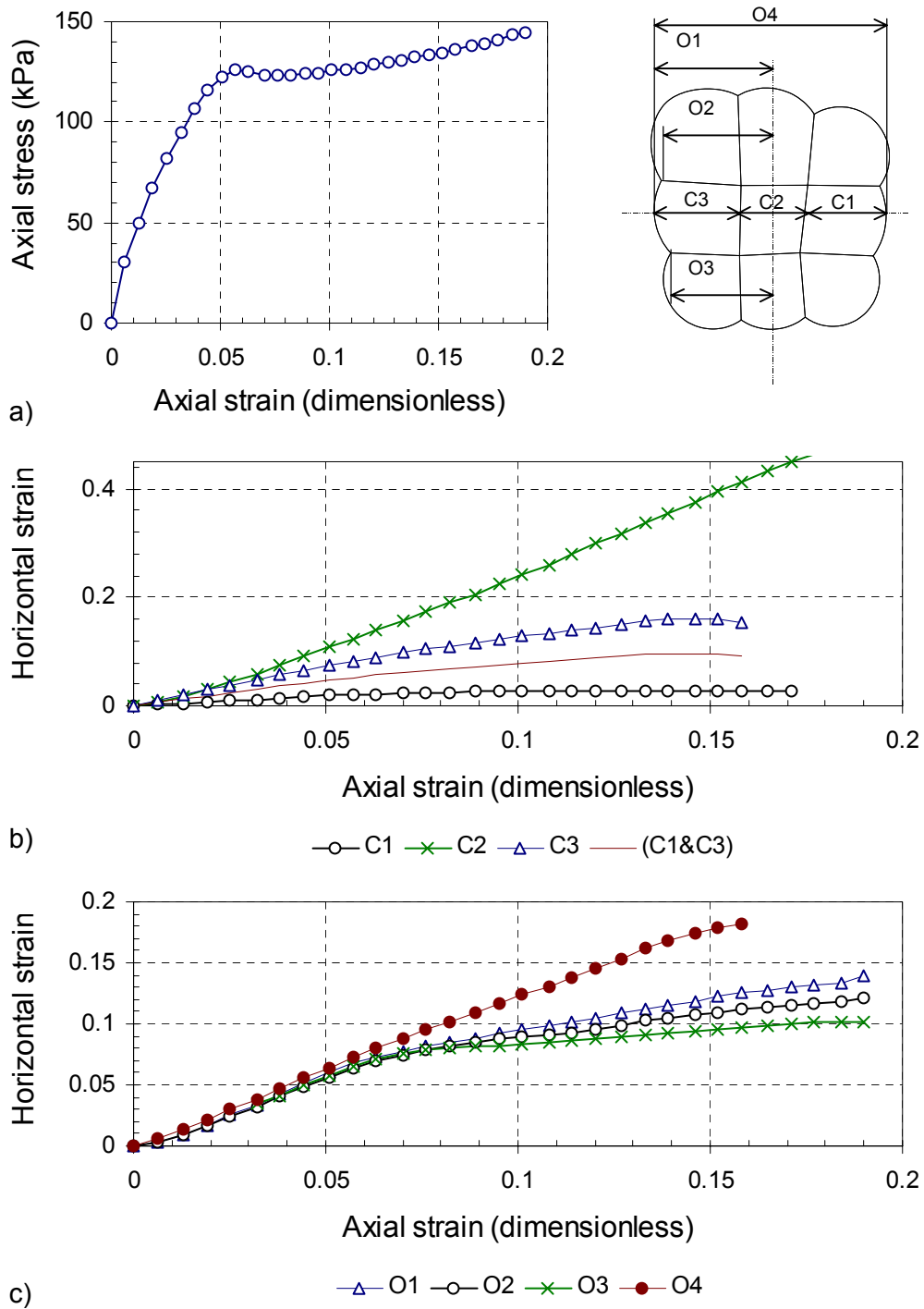


Figure 3.39 Results of the compression test on the 3x3 cell pack.

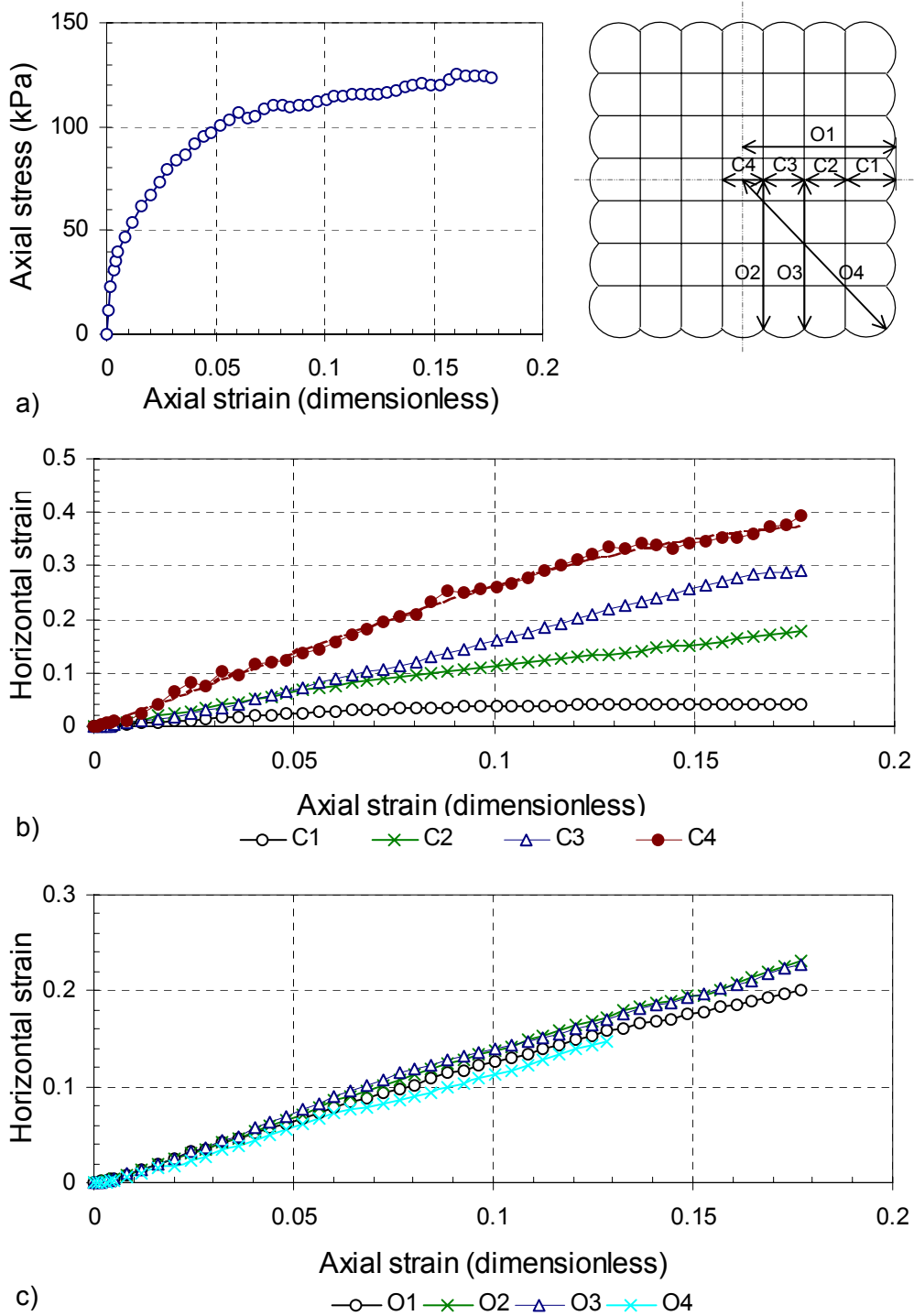


Figure 3.40 Results of the compression test on the 7x7 cell pack.



Figure 3.41 The 3x3 cell pack after compression.



a) after 20% axial strain



c) after 40% axial strain

d) top surface after 40% axial strain

Figure 3.42 The 7x7 cell pack after compression.

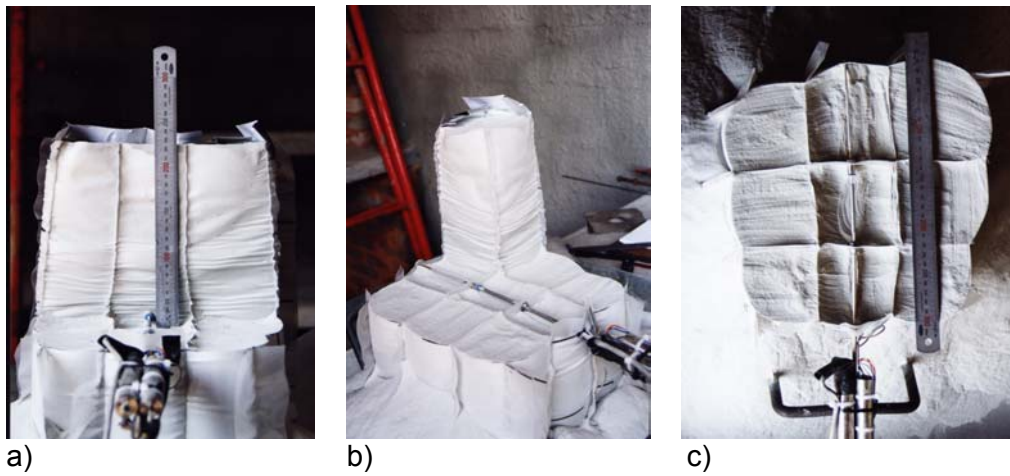


Figure 3.43 Internal geometry of the 3x3 pack after tests.

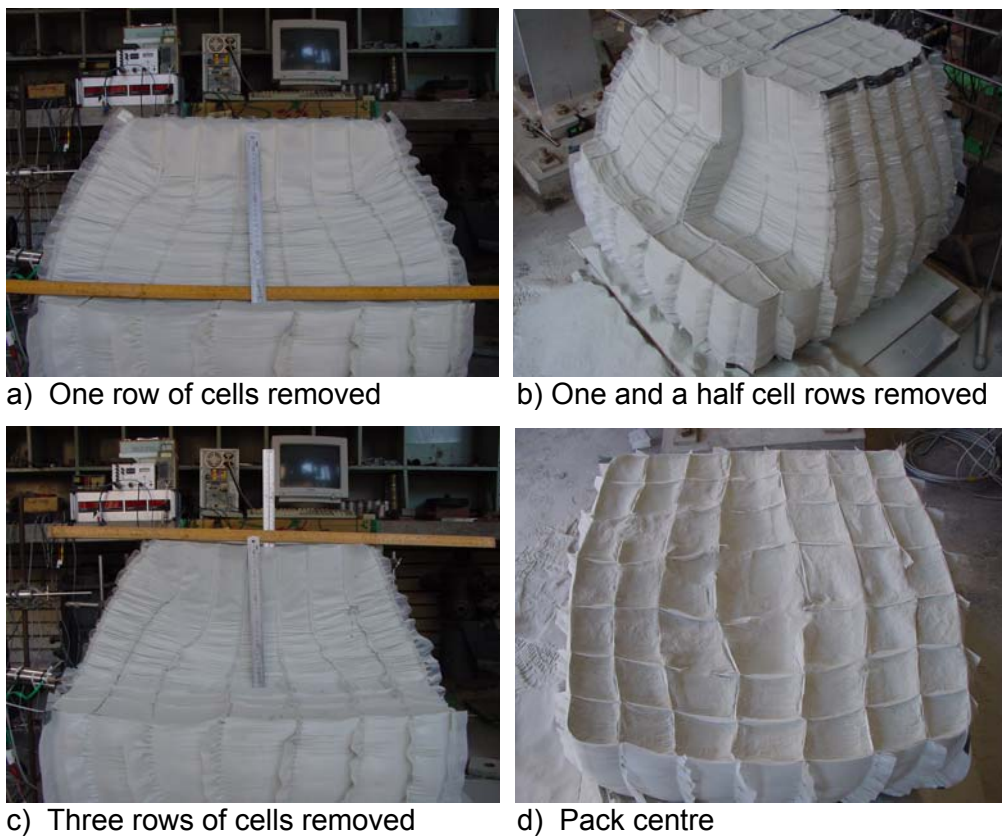
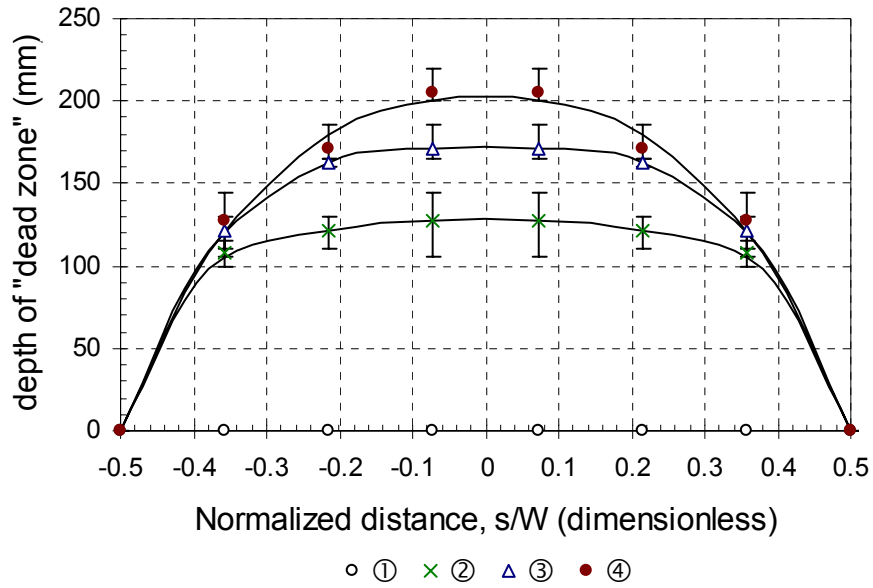
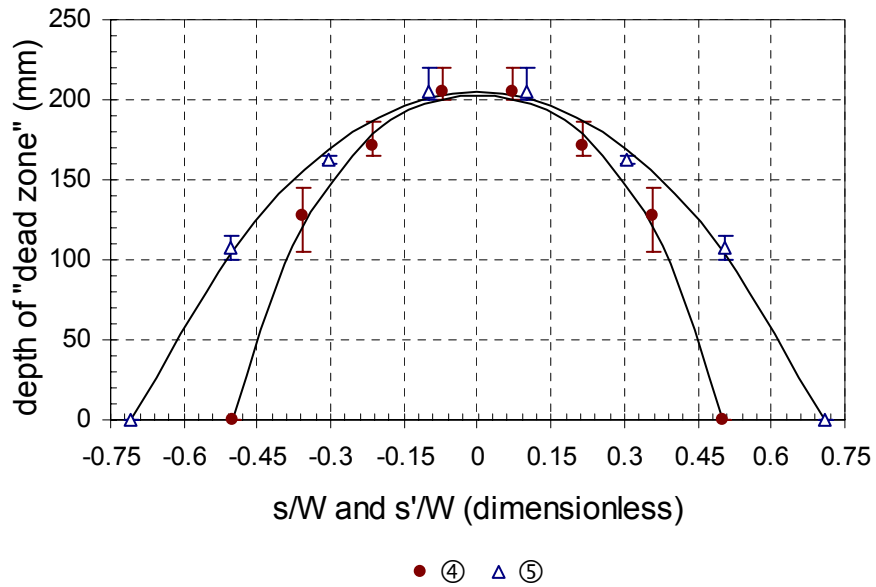


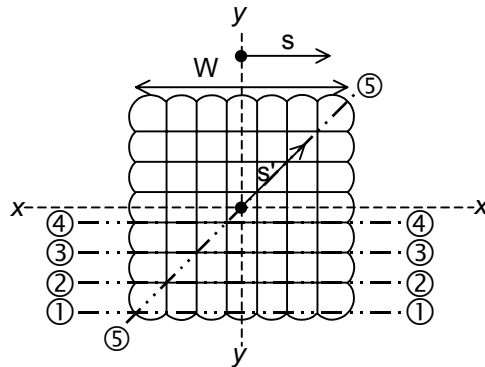
Figure 3.44 Internal geometry of the 7x7 pack after tests.



a)



b)



c)

Figure 3.45 The measured extent of the "dead zone" after completion of the test on the 7x7 cell pack.